

# Temperature-Dependent Charge Transport and Hall Effect Behavior in MoS<sub>2</sub> Nanostructures in (270–345)°K Temperature Range

Hussein AlHussein<sup>a,\*</sup> 

<sup>a</sup>Department of Physics, Faculty of Science, University of Aleppo, Syria.

## Keywords:

Molybdenum disulfide (MoS<sub>2</sub>)  
Nanostructures,  
Hall effect  
Quantum transport  
Thermally activated carrier  
Charge carrier mobility  
Magnetic transport

## \* Corresponding author:

Hussein AlHussein  
E-mail: [husianphy990@gmail.com](mailto:husianphy990@gmail.com)

Received: 10 March 2026

Revised: 14 April 2026

Accepted: 16 May 2026



## ABSTRACT

*This study systematically explores the thermal transitions in electron transport mechanisms within molybdenum disulfide (MoS<sub>2</sub>) nanostructures and sheets in the 270–345 °K thermal range, using four-probe Hall effect measurements under a static magnetic field of 0.5 T. The study aims to determine the nature of the dominant transport mechanisms, analyze the transitions between localized and diffuse regimes, and assess the likelihood of quantum transitions in this near-room-temperature thermal range. Electrical measurements revealed non-uniform thermal behavior, indicating the presence of three distinct transport regions. In the lower thermal range (270–285 °K), a localized transport regime characterized by high resistivity, low carrier density, and low mobility prevailed, consistent with variable-range hopping (VRH) mechanisms and weak localization effects resulting from structural defects and surface states. In the intermediate range (285–305 °K), a clear thermal transition was observed, characterized by a sharp decrease in resistivity and a nonlinear change in conductivity, accompanied by a possible reversal in the Hall effect. This behavior suggests a redistribution of electron density with increasing thermal activation of the carriers. In the higher thermal range (305–345 °K), transport became primarily limited by phonon scattering. Conductivity stabilized relatively, and mobility gradually decreased with increasing temperature, while the Hall effect approached zero due to the increasing compensation between the carriers. These results confirm that the observed behavior reflects a gradual thermal transition between different transport regimes, governed by competition between quantum localization, thermal activation, and phonon scattering.*

© 2026 Journal of Materials and Engineering

## 1. INTRODUCTION

Two-dimensional materials are an ideal platform for studying quantum electronic phenomena and carrier-phonon interactions, thanks to their

characteristic dimensional confinement and the structural changes that occur when the layer thickness is reduced to the atomic scale. Among these materials, molybdenum disulfide (MoS<sub>2</sub>) stands out. It is a semiconductor from the family of

transition metal dichalcogenides (TMDs) that features a controllable energy gap, high chemical stability, and a variety of crystalline phases, making it a model material for studying electron transport and quantum transitions in two-dimensional systems [1,2]. MoS<sub>2</sub> consists of atomic layers that are internally bonded by strong covalent bonds, while the layers are stacked via weak van der Waals forces, allowing for easy layer separation and control over the number of layers. With the transition from bulk to monolayer, the energy gap shifts from indirect (~1.2 eV) to direct (~1.8 eV), rearranging the positions of the valence and conduction bands and directly affecting the electron transport behavior [3,4]. MoS<sub>2</sub> exhibits several crystalline phases, most notably the hexagonal 2H phase, characterized by semiconducting behavior and high thermal stability, and the metallic 1T phase, which is characterized by the absence of an energy gap and high conductivity. Additionally, there is the distorted 1T' phase, associated with lattice distortions that can lead to topological states and quantum transitions under certain conditions. The structural transition between these phases (2H ↔ 1T) is a model for studying the effect of the crystalline phase on the electronic structure and the transition from a semiconductor to a metallic state [5,6].

The electron transport mechanisms in MoS<sub>2</sub> depend on a complex interaction between carriers, phonons, structural defects, and quantum confinement. At near-room temperatures, band transport dominates the conductivity behavior, with mobility decreasing with increasing temperature due to phonon scattering. Thermally activated conduction, on the other hand, is observed in samples with lattice defects or impurities [7,8]. At lower temperatures or in very thin two-dimensional samples, quantum mechanisms such as variable range hopping and weak localization may prevail, reflecting the effects of dimensionality confinement and electron wave interference. Furthermore, a metal-insulator transition may arise from the interaction of these factors; this is an intrinsic transition that can be detected by conductivity and Hall effect measurements [9,10]. Hall effect measurements play a crucial role in studying these systems, providing precise information about the type and concentration of carriers, mobility, and the nature of the electron transport transitions. By analyzing the thermal behavior of the conductivity and Hall modulus within the thermal range (270–345 °K), transitions from thermal band transport to

hopping transport can be distinguished, in addition to revealing subtle structural shifts and their impact on electrical properties. Understanding the relationship between crystal structure and transport mechanisms in MoS<sub>2</sub> forms the basis for the design of high-performance electronic and nanoelectronic devices and provides a precise experimental framework for studying quantum and thermal transitions in two-dimensional systems [11-13].

Accordingly, this work aims to present a comprehensive study of electronic transitions in MoS<sub>2</sub> nanostructures in the temperature range (270–345 °K) using magnetic Hall measurements, with a detailed analysis of the results to understand the mechanisms of electronic transport, thermal dispersion, and charge carrier density and mobility changes across this range.

## 2. SIGNIFICANCE OF THE RESEARCH

Studying the electronic properties and quantum transitions of molybdenum disulfide is fundamental to understanding electronic transport in two-dimensional systems and the transitions between their different crystalline phases. These studies provide a basis for developing advanced nanoelectronic devices, such as transistors, highly sensitive sensors, and optical devices. Hall effect measurements allow for the analysis of charge carrier concentration and mobility, and the detection of transitions between thermal and quantum transport mechanisms with high precision. This research also contributes to enriching theoretical models of quantum physics and understanding the effects of dimensionality confinement and the interactions between charge carriers and phonons in semiconductors.

## 3. EXPERIMENTAL AND PRACTICAL STUDIES

### 3.1. Instruments and equipment

1. HMS-5000 Hall effect spectrometer.
2. Atomic force microscope (AFM).
3. Leybold Didactic X-ray spectrometer (XRD), model 81-554.
4. Carbolite CWF 1200 heat treatment furnace.
5. PMC 502p-2 magnetic mixer with heater.
6. SMIC autoglaze.
7. Chemical preparation equipment.

### 3.2 Preparation method

To prepare MoS<sub>2</sub> nanostructures, the synthesis process was carried out using the hydrothermal method. In typical MoS<sub>2</sub> nanoparticle synthesis processes, sodium sulfide is used as the sulfur source to obtain molybdenum sulfide through chemical reactions. [14] The preparation stages can be divided into the following steps: 1.235 g of ammonium heptamolybdate tetrahydrate ((NH<sub>4</sub>)<sub>6</sub>Mo<sub>7</sub>O<sub>24</sub>·4H<sub>2</sub>O) was placed in 25 mL of distilled water with continuous stirring. After 30 minutes, 0.5 g of citric acid monohydrate (C<sub>6</sub>H<sub>8</sub>O<sub>7</sub>·H<sub>2</sub>O) was added to the solution. Next, 0.31 capacity of sodium sulfide (Na<sub>2</sub>S) crystals were added to the solution mixture. The solution was then transferred to a sterilizer at 200 °C for 6 hours. It was then cooled naturally to room temperature. The final black product was washed with ethanol and then with distilled water. The resulting powder was dried at 70°C. A 1 g portion of the powder was then pressed using a hydraulic press at a cap acity of (5 tons/cm<sup>2</sup> ) to obtain a tablet with a diameter of (14 mm) and a thickness of (3 mm), as shown in Figure 1.



Fig. 1. Shows a sample of the prepared molybdenum disulfide.

### 3.3 X-ray diffraction spectrum

X-ray diffraction (XRD) spectra of the prepared tablets of (MoS<sub>2</sub>) showed the presence of clear crystallization peaks, as X-ray diffraction measurements showed a peak corresponding to the crystal plane (002) opposite the angle (2θ = 14.6°), which characterizes molybdenum sulfide layers in their single or multiple phases, as shown in Figure 2. This is consistent with the reference cards for molybdenum disulfide (PDF#75-1539) [15].

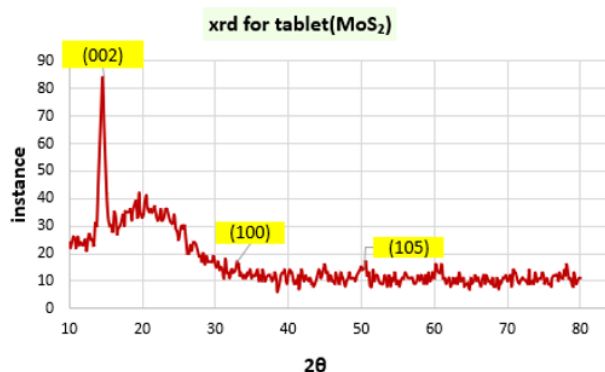


Fig. 2. Shows the X-ray spectrum of (tablets-MoS<sub>2</sub>) sample.

Based on Bragg's law of X-ray diffraction, as in equation (1), the distance between crystal planes defined by Miller indices (hkl) can be determined as:

$$2d_{hkl} \sin(\theta_{hkl}) = n\lambda \quad (1)$$

where:  $d_{hkl}$  represents the distance between parallel crystal planes along the hkl direction,  $\theta_{hkl}$  is the angle of diffraction,  $n$  is the order of diffraction, and  $\lambda$  represents the wavelength of the X-rays ( $\lambda = 1.541 \text{ \AA}$ ), where  $\theta$  is the mid-intensity width of each peak, measured in radians. Calculation shows that  $d_{hkl} = 5.25 \text{ \AA}$

### 3.4 Study of the surface structure of molybdenum disulfide (MoS<sub>2</sub>) tablets using atomic force microscopy (AFM)

An AFM image was taken of the surface of a tablet prepared from molybdenum disulfide powder (MoS<sub>2</sub>). We used measurements of the same area of the sample surface (1.02 μm × 1.02 μm), as shown in Figure 3.

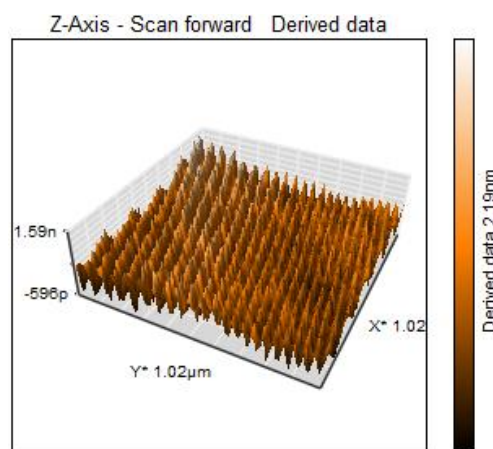


Fig. 3. AFM images of the surface of a molybdenum disulfide (MoS<sub>2</sub>) tablet prepared to a scale of (1.02μm × 1.02μm).

The AFM image shows the presence of uniform nano-aggregates on the surface. The lateral size of the aggregations ranges from (1000 nm) to (15-20 vertices), which represents the diameter or width of the aggregations. This indicates that the surface aggregation size is (50-100 nm), while the vertical height values range from (-596pm, 1.59nm) represents the surface roughness and ranges from (1-2 nm), meaning the nano-terrain is very small (Low Roughness Range). This indicates a thin layered structure, meaning the sample has a high-density nanostructure. This means that the (2H/1T-MoS<sub>2</sub>) structure is multilayered (Few-Layer to Multilayer), and the (2H/1T-MoS<sub>2</sub>) aggregates are in the form of nano-packs with active edge sites resulting from the arrangement of the (2H/1T-MoS<sub>2</sub>) layers during the hydraulic pressing process.

### 3.5 Studying sheet resistance changes with temperature

The sheet resistance curve shows three distinct thermal regions between (270–345 °K), reflecting the changing electron transport mechanism in MoS<sub>2</sub> nanosheets. As illustrated in Figure 4, in the lower temperature range (270–280 °K), the resistance is very high and decreases rapidly with increasing temperature. This indicates a small number of free charge carriers and that a significant portion of electrons are trapped in impurity levels or localized surface states. In this region, hopping conduction or Variable Range Hopping (VRH) dominates. As the temperature increases, the charge carriers gradually release from their localized levels, causing the resistance to decrease almost exponentially. This behavior is typical of the charge carrier freeze-out regime in semiconductors.

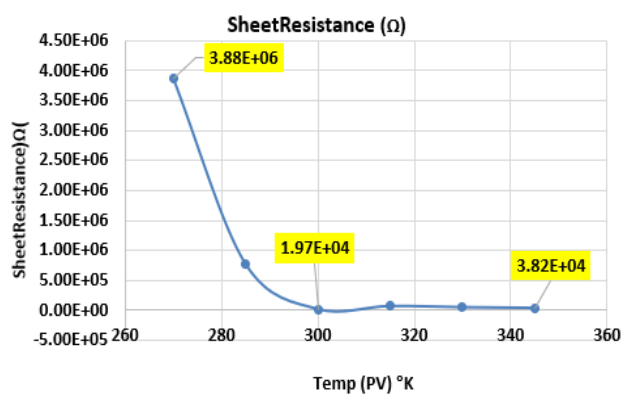


Fig. 4. Shows changes in sheet resistance with temperature.

In the intermediate range (270–300 °K), a sharp drop in sheet resistance occurs, indicating a clear transition from localized to band-like transport. In this region, strong thermal activation of the carriers occurs, with their density increasing significantly, as evidenced by Hall measurements. This behavior can be approximated by the Arrhenius equation  $R_S \propto \frac{E_a}{e^{kT}}$ , making this region suitable for extracting the activation energy  $E_a$  associated with impurity levels or the effective gap.

In the higher thermal range (300–345 °K), the sheet resistance stabilizes relatively at lower values with minimal variations, indicating that most charge carriers are now thermally activated, and that the dominant factor in transport is no longer the number of charge carriers but their mobility. At this stage, the scattering of lattice phonons increases with increasing temperature, leading to a decrease in mobility  $\mu$  in an almost inverse relationship with T. Thus, even with a slight increase in the concentration of n-type carriers, the resistance remains quasi-stable due to the balance between increasing n and decreasing  $\mu$ . This behavior is characteristic of the phonon (phonon-limited regime) in two-dimensional semiconductors.

### 3.6 Study of electrical conductivity ( $\sigma$ ) changes with temperature

The electrical conductivity curve exhibits non-uniform thermal behavior, reflecting the competition between charge carrier concentration and mobility according to the relationship  $\sigma = qn\mu$ . In the low temperature range (270–280 °K), conductivity is very low, which corresponds to a scarcity of free charge carriers due to their freezing in impurity levels or local states close to the Fermi level. In this region, transport is controlled by local mechanisms such as hopping conduction, where both the charge density n and mobility  $\mu$  are limited, leading to quasi-insulating conductivity values, as illustrated in Figure 5.

Upon reaching the intermediate temperature range (280–290 °K), a sharp increase in conductivity occurs, reaching a relatively high value, indicating efficient thermal activation of the carriers. At this stage, electrons are released from shallow impurity levels or edge states in the nanosheets, and a gradual transition from localized to band conduction takes place. This sudden increase can be explained as a result of a rapid increase in charge carrier concentration that outweighs any potential decrease in mobility.

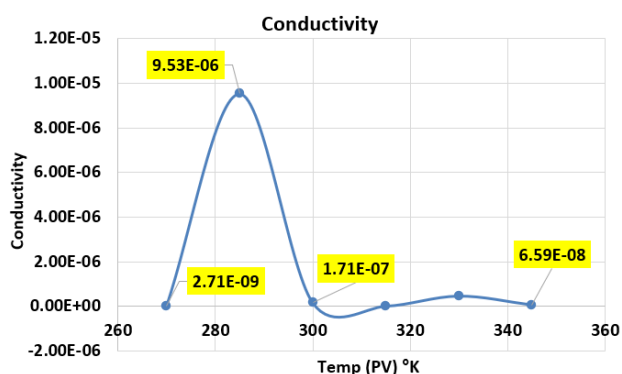


**Fig. 5.** Changes in electrical conductivity ( $\sigma$ ) with temperature changes.

However, as the temperature approaches 300 °K and beyond, conductivity decreases again, and slight fluctuations appear with increasing temperature. This behavior reflects the onset of lattice phonon scattering dominance, where the vibrations of the crystal lattice increase with temperature, leading to a decrease in mobility  $\mu$ , approximately expressed as ( $\mu \propto T^{-m}$ ). Although the number of charge carriers continues to increase with temperature, the decrease in mobility becomes the dominant factor, explaining the relative decrease in conductivity in this thermal range. This behavior is typical in two-dimensional materials, where the effect of surface and phonon scattering is more pronounced compared to volumetric materials.

### 3.7 Studying volumetric resistivity ( $\rho$ ) changes with temperature

The volumetric resistivity curve reflects the inverse behavior of conductivity according to the relationship  $\rho = 1/\sigma$ . However, its physical analysis provides important indicators about the nature of the transport. At 270 °K, the resistivity registers a very high value, indicating that the material at this stage is close to insulating behavior, as shown in Figure 6, and that the transport does not occur through extended bands but rather through localized states associated with impurities or structural defects. In the thermal range (280-300 °K), the resistivity drops sharply, confirming the occurrence of heat transfer in the transport mechanism. This significant decrease indicates that the charge carriers have overcome an energy barrier associated with impurity levels or an effective energy gap, allowing them to transition to extended states within the conduction band. This range represents the transition stage from an activation-controlled transport system to a more metalloidal system.

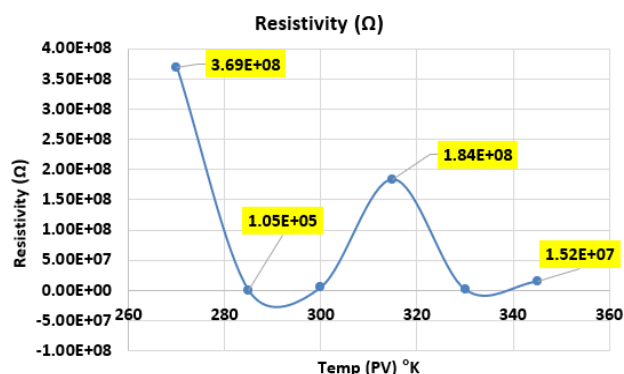


**Fig. 6.** Changes in volumetric resistivity ( $\rho$ ) with temperature changes.

At higher temperatures (300–320 °K), a second relative increase in resistivity appears, a non-uniform behavior reflecting the complexity of transport mechanisms in nanosheets. This peak can be explained by increased phonon scattering or by a change in the dominant carrier type due to the interference of electron and hole contributions. In two-dimensional materials, surface and edge states may play an additional role in the redistribution of charge carrier density, leading to this non-uniform behavior. Subsequently, as the temperature continues to rise up to 320 °K, the resistivity tends to decrease again, indicating an additional thermal contribution from the (intrinsic carriers).

### 3.8 Study of bulk carrier concentration (n) changes with temperature

The carrier concentration curve derived from Hall measurements is the most indicative of the transport nature and the dominant carrier type. In the lower temperature range (270-285 °K), the values of n are relatively small, indicating a limited carrier density, which corresponds to the freezing zone of charge carriers, as shown in Figure 7. A positive sign in this region suggests the predominance of holes or a weak contribution from acceptor impurities.

Upon transitioning to the intermediate range (285–300 °K), a clear change in the value and notation of n is observed, potentially indicating a reversal in the Hall effect signal. This signal change is a significant indicator of a shift in the dominant carrier type, i.e., a transition from p-type to n-type behavior or vice versa. This typically occurs when the position of the Fermi level changes with temperature or when donor impurity levels begin to contribute more actively to transport.

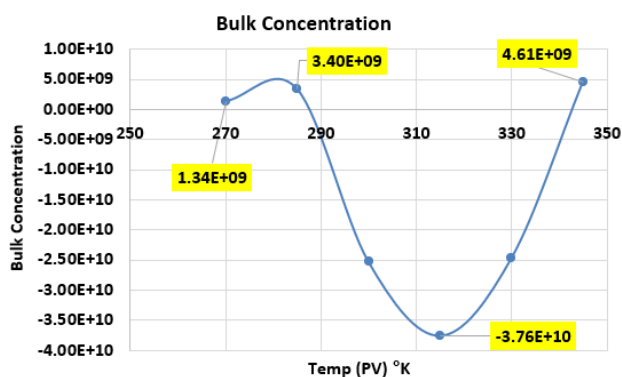


**Fig. 7.** Shows changes in the concentration of charge carriers (bulk carrier concentration,  $n$ ) with changing temperatures.

In the higher thermal range (300–330 °K), the value of  $n$  increases markedly with a clear dominance of a single carrier type (as evidenced by the negative signal in the data), indicating that the conduction band has become the primary source of free carriers. This reflects a transition to a transport regime closer to phonon-limited semimetallic behavior. However, a return to a positive signal at the highest temperature (345 °K) suggests the possibility of mixed conduction or simultaneous contribution of electrons and holes. In MoS<sub>2</sub> nanosheets, this phenomenon could arise from the influence of surface states, the repositioning of the Fermi level, or the activation of deep impurity levels. At high temperatures.

### 3.9 Study of magnetoresistance changes with temperature

Measurements of molybdenum disulfide (MoS<sub>2</sub>) in the temperature range of (270–345 °K) indicate distinct changes in magnetoresistivity behavior with temperature. This behavior can be divided into three distinct temperature regions. In the lower temperature range of (270–285 °K), magnetoresistivity exhibits very high values, reaching approximately  $2.63 \times 10^8$  at 270 °K, and then begins to decrease sharply with a slight increase in temperature. This behavior suggests that the electron transport mechanism in this region is subject to significant quantum effects. At low temperatures, the coherence of the electron phase is strong, and the scattering is relatively weak, allowing phenomena such as weak localization or variable range hopping to occur. In this case, the magnetic field significantly influences the overlapping electron paths, resulting in very high magnetoresistivity. As the temperature increases, this quantum effect begins

to diminish. Rapidly, the magnetic resistance decreases significantly, as shown in Figure 8. In the intermediate range (285–305 °K), the magnetic resistance continues to decrease until it reaches very small values near (305–315 °K). In this region, phonon scattering (collisions of electrons with crystal lattice vibrations) begins to dominate the transport mechanism.

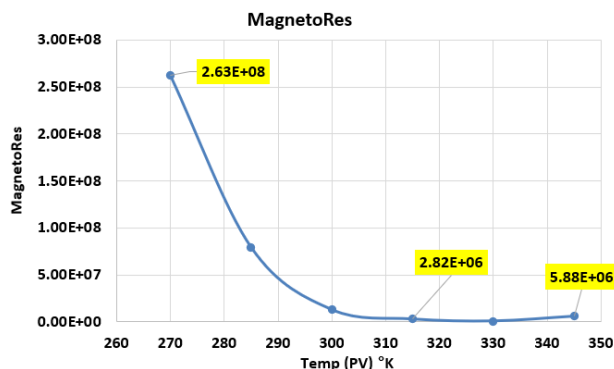


**Fig. 8.** Changes in magnetic resistance (magnetoresistance) with temperature changes.

This leads to a decrease in phase coherence length and weakens quantum interference effects, causing the system to gradually transition from a quasi-local transport mode to a diffusive transport mode. This region represents a clear transport crossover between two different electron transport modes. At higher temperatures (305–345 °K), a slight increase in magnetoresistance is observed after it has reached its lowest values. This increase can be explained by the increased phonon influence with rising temperature, which enhances scattering processes and modifies the transport mechanism. Additionally, thermal carrier activation may begin to appear, leading to a change in carrier density or their energy distribution within the energy bands. These factors combined result in a slight re-increase in magnetoresistance, but it remains significantly lower than its values at lower temperatures. Overall, this behavior reflects a gradual transition from a system dominated by quantum phenomena at lower temperatures to one dominated by phonon scattering and diffusive transport at higher temperatures, with a clear transition region between the two.

### 3.10 Studying mobility changes with temperature

Mobility exhibits a clear nonlinear behavior with temperature changes and can be divided into three main regions. In the low thermal

range (270–285 °K), the mobility starts at a relatively low value of approximately 0.126 at 270 °K and then rises sharply to a maximum value of approximately (175 at 285 °K). This abrupt increase indicates a significant improvement in the carriers' ability to move within the material. In this region, the system may be affected by defects or localized states at the lowest temperatures. As the temperature increases, partial activation of the carriers occurs, reducing the effect of localized confinement and increasing the number of carriers capable of participating in transport. The response may also improve due to the release of carriers from shallow energy traps. This thermal point represents an equilibrium between a suitable carrier density and a still low phonon dispersion level, resulting in the highest value of mobility, as illustrated in Figure 9.

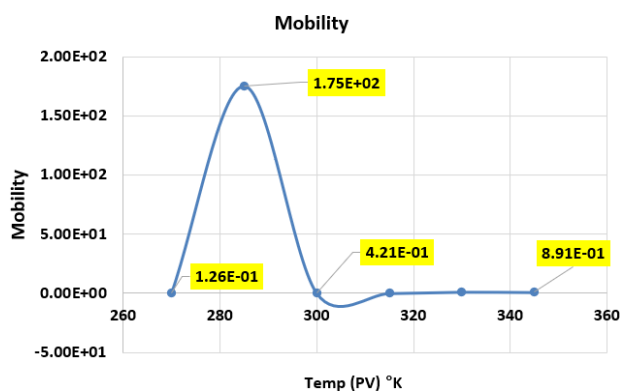


Fig. 9. Study of mobility changes with temperature.

In the medium range (285–300 °K), the mobility collapses sharply after reaching The peak. This decrease is associated with a marked increase in phonon scattering with rising temperature. The increased vibrations of the crystal lattice reduce the relaxation time of the carriers, and consequently, the mobility decrease. Here, the effect of phonons begins to overcome any improvement resulting from an increased number of carriers. In the higher temperature range (300–345 °K), the mobility remain very low with only minor changes. This indicates that transport has become almost entirely governed by thermal scattering, and the system has entered a conventional diffusive transport regime, where the mobility are primarily limited by carrier-phonon collisions. Overall, the kinetic behavior reflects an optimal thermal window near (285 °K) achieving the highest transport performance, followed by a regime dominated by thermal scattering processes.

### 3.11 Studying changes in the V/H ratio with temperature

The V/H ratio exhibits more complex behavior, with the signal changing from negative to positive within the studied range, indicating a change in the type or nature of the dominant carriers. In the thermal range (270-315 °K), the ratio remains negative with gradual changes. The negative signal usually indicates that the dominant carriers are (n-type) electrons. In this region, transport appears to occur through a single, relatively dominant electron channel, with limited changes in the carrier type, as shown in Figure 10.

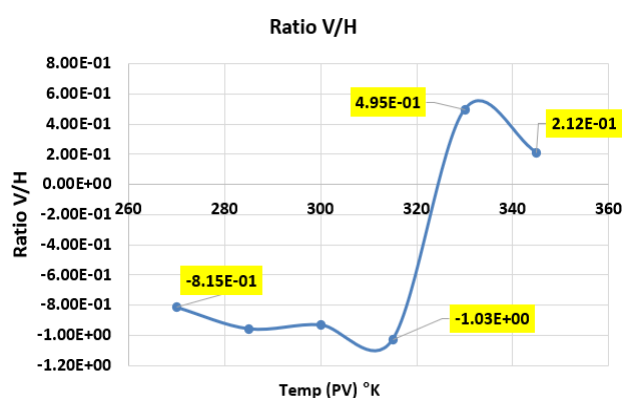


Fig. 10. Studying changes in the V/H ratio with temperature.

At the range (315-330 °K), a sharp change in behavior occurs, with the signal reversing from negative to positive. This transition represents a very important transition point in the system. The signal reversal often indicates one of the following possibilities:

- A change in the type of dominant carriers from electrons to holes.
- The presence of two transport channels (electrons and holes) with a change in the dominance of one due to activation. Thermal.
- A shift in the transport mechanism or a change in the position of the Fermi level due to thermal activation. In the higher range (330–345 °K), the ratio remains positive with a slight decrease after reaching a maximum value. This indicates a relative stabilization of the dominance of a new type of carrier (often holes), or a new equilibrium between multiple transport channels.

### 3.12 Analysis of the thermal behavior of charge carrier density in molybdenum disulfide (MoS<sub>2</sub>) nanostructures

The charge carrier density in molybdenum disulfide (MoS<sub>2</sub>) nanostructures was measured using the Hall effect between different electrode pairs (BD Hall and AC Hall), in addition to calculating the overall average, within the thermal range of 270–345 °K. The results showed nonlinear thermal behavior reflecting the complexity of electron transport mechanisms in this thermal range close to room temperature.

#### 3.12.1 Study of the change in n carrier density (BD Hall) between the two electrodes (B, D)

In the low thermal range (270–285 °K), the carrier density registers relatively high values, reaching approximately  $9.28 \times 10^9$  at (270 °K). This indicates a clear dominance of active charge carriers, likely electrons, demonstrating n-type semiconductor behavior in this thermal region. MoS<sub>2</sub> nanostructures may exhibit surface states or donor-like defects that contribute to increased carrier concentration at low temperatures, as illustrated in Figure 11.

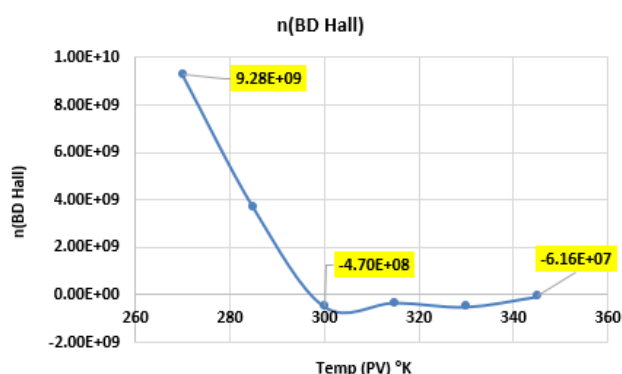


**Fig. 11.** Study of n-carrier density changes (BD Hall effect) with temperature changes.

As the temperature rises to approximately 300 °K, a sharp decrease in carrier density occurs, reaching very low values. A slight negative signal appears near 300–310 °K, with a value of approximately  $-4.7 \times 10^{-8}$ . This sharp change indicates an important thermal transition point in the system. This behavior can be explained by one of the following scenarios:

- A transition in the dominant carrier type.
- A temporary carrier compensation between electrons and holes.

- A change in the position of the Fermi level due to thermal activation and redistribution of carriers between the valence and conduction bands.

After 330 °K, the carrier density begins to rise again, reaching approximately  $6.16 \times 10^7$ , indicating the onset of thermal activation of additional carriers or the release of carriers from deeper energy levels. Cooling

#### 3.12.2 Study of charge carrier density changes (AC Hall) between electrodes (A, C)

Measurements between the AC electrodes show partially different thermal behavior, reflecting the possibility of spatial heterogeneity in the carrier distribution within the sample. In the range of (270–310 °K), the carrier density remains relatively low with slight changes, as shown in Figure 12.

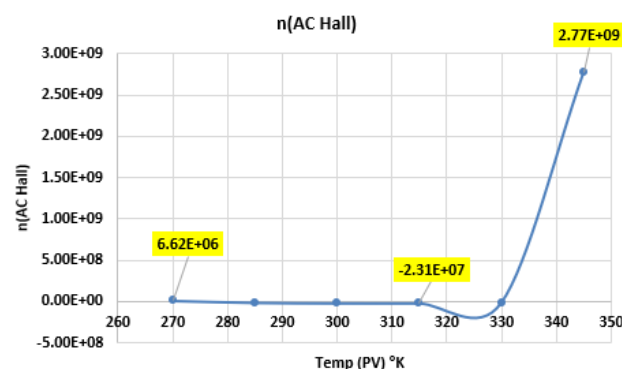


**Fig. 12.** Study of changes in carrier density n (AC Hall) with temperature changes.

At approximately (320 °K), a small negative value ( $-2.31 \times 10^7$ ) appears, supporting the hypothesis of a carrier transition or the presence of two competing transport channels in this thermal region. At higher temperatures (340–345 °K), a sharp increase in carrier density occurs, reaching approximately ( $2.77 \times 10^9$ ). This behavior indicates strong thermal activation or the dominance of a different transport channel at this measurement direction, which is expected in nanostructures due to edge effects, structural stress, or a different defect distribution.

#### 3.12.3 Study of average charge carrier density changes contributing to the hall potential (n)

When studying the overall average charge carrier density, a clear transitional behavior emerges, which can be divided into three thermal regions, as shown in Figure 13.

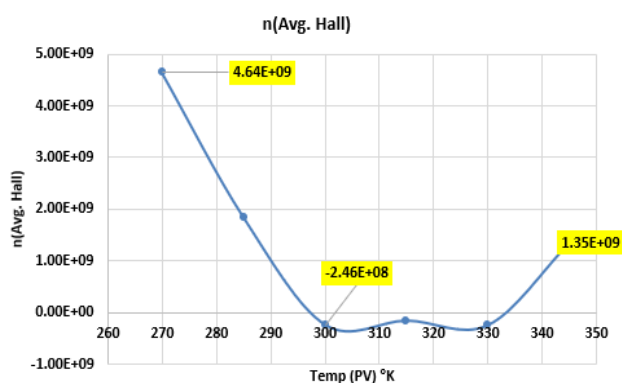


**Fig. 13.** Study of carrier density changes (avg. Hall) with temperature changes.

High value at (270 °K) equals  $(4.6 \times 10^9)$  Gradual decrease to a small negative value near (300 °K) equals  $(-2.46 \times 10^8)$ , Returns to an increase to  $(1.35 \times 10^9)$  at (340-345 °K) The (300-320 °K) range represents a transport transition region, where the system appears to be undergoing compensation between two carrier types or a transition in the transport mechanism from a single-carrier to a multi-channel system. The above results reflect the characteristic behavior of MoS<sub>2</sub> nanostructures, where the following factors play a crucial role.

The effect of nanoscale dimensions and increasing surface-to-volume ratio. The presence of structural defects and local energy levels. Gradual thermal activation of the carriers. The possibility of two-carrier transport. The difference in results between BD and AC also indicates spatial inhomogeneity in the Hall response. This is common in two-dimensional materials and nanostructures due to edge effects, grain boundaries, and lattice stress.

### 3.13 Study of hall potential changes in molybdenum disulfide (MoS<sub>2</sub>) with temperature

Molybdenum disulfide (MoS<sub>2</sub>) is a two-dimensional material with a layered structure. The bonds in this layered structure are strong horizontally within the layers (Mo-S), but weak vertically between the layers due to van der Waals forces. Consequently, electrical conduction is dependent on these bonds and is characterized as anisotropic (not directionally uniform) and highly sensitive to the number of layers, defects, cooling, and magnetic field. Therefore, potential measurements between different points are not identical. We took four electrodes from the surface

of a molybdenum disulfide disk, forming four points (A, B, C, D) in a square with a distance of 1 cm between each point, as shown in Figure 14.

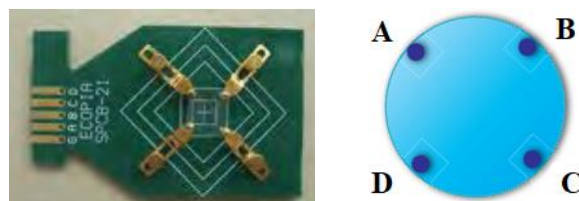


**Fig. 14.** Shows the position of the electrodes for measuring electrical potential.

The quadrilateral geometry of the points (A, B, C, D) is distributed around the perimeter of the sample as shown in Figure 14. The electrical potential between each pair of points is measured as  $(V_{AB}, V_{AC}, V_{BC}, V_{CD}, V_{BD}, V_{DA}, V_{(HALL, average)})$ . Each time a perpendicular current is applied, the transverse potential is measured. For example, if the current is applied ((A → C), the transverse Hall potential is (B ↔ D).

#### 3.13.1 Hall potential change for the AB electrode

The Hall potential behavior of molybdenum disulfide (MoS<sub>2</sub>) nanostructures was investigated under a thermal range of 270–345 °K and a constant magnetic field of 0.5 T. The results showed a significant change in the value and signal of the Hall potential with increasing temperature, particularly in the thermal range of 300–320 °K, indicating a change in the electrical transport mechanism within the sample. At relatively low temperatures (270–300 °K), large, positive Hall potential values were observed in some measurement directions, indicating the dominance of positive charge carriers (holes) in the transport process. In MoS<sub>2</sub> nanomaterials, this behavior can be explained by the presence of surface energy states and dense grain boundaries, leading to partial electron confinement or the generation of levels close to the valence band, thus promoting seemingly p-type behavior. Furthermore, the decrease in the density of active carriers in this thermal field leads to a higher Hall effect and consequently an increase in the measured Hall potential, as shown in Figure 15.

As the temperature increases and approaches the 310–320 °K range, a sharp decrease in the Hall potential is observed, sometimes approaching zero or exhibiting a change in sign. This behavior

is attributed to the gradual thermal ionization of impurity levels or local states within the energy gap, leading to the release of additional electrons and increasing their contribution to the transport process. At this stage, the system enters a two-carrier transport regime, where the electron and hole densities converge. As a result, the Hall effect decreases significantly because its value depends on the difference between the two charge carrier concentrations, and when  $n \approx p$ , the Hall effect approaches zero.

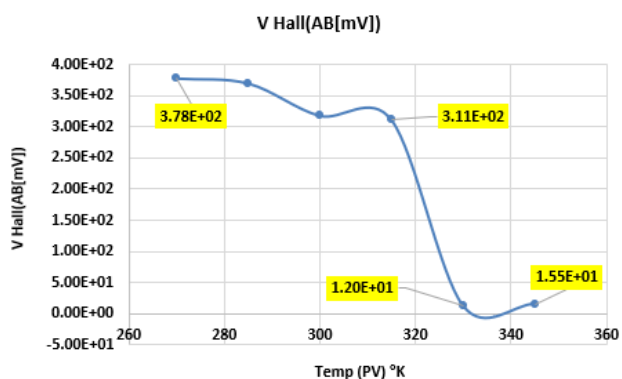


**Fig. 15.** Hall potential changes for electrode (AB) with temperature change.

At temperatures above 320 °K, the Hall potential stabilizes at relatively small values, indicating a transition to a more diffusive band transport regime. In this thermal field, sufficient thermal energy is generated to reduce the barrier effect at the grain boundaries and enhance the electronic interconnection between nanoparticles. Consequently, transport becomes less influenced by local states and more subject to band transport.

It is important to note that the applied magnetic field (0.5 T) is insufficient to exhibit the quantum Hall effect in this high thermal field, as the thermal energy at room temperature (~25 meV) far exceeds the expected Landau level separation at this field. Furthermore, the absence of quantum plateaus or sharp jumps in the data supports the conclusion that the observed changes do not represent a quantum phase transition, but rather reflect a thermal shift in the transport mechanism resulting from carrier redistribution and a change in the contribution of local states to the nanostructure.

Based on this, it can be concluded that the thermal behavior of the Hall potential in nano-MoS<sub>2</sub> within the range (270-345 °K) and under a magnetic field (0.5 T) reflects a gradual transition from a transport regime controlled by surface states and

granular boundaries to a two-carrier transport regime and then to a more diffuse band transport, without evidence of a true quantum Hall transition under these experimental conditions.

### 3.13.2 Change in hall potential for the BC electrode

Measurements between the two BC electrodes showed significant negative Hall potential values at low temperatures (270–290 °K), indicating the dominance of electrons as the principal charge carriers (n-type behavior). The occurrence of this behavior in MoS<sub>2</sub> nanomaterials is consistent with the n-type semiconductor nature, which is often attributed to the presence of sulfur vacancies acting as sources of free electrons. As the temperature gradually increased, a rise in the Hall potential (i.e., a decrease in the absolute negative value) was observed, indicating a decrease in the influence of the dominant electrons or an increase in the contribution of positive carriers. In the thermal range (300–320 °K), the Hall potential approaches zero, reflecting a gradual transition from a single-carrier to a two-carrier transport regime, where the electron and hole densities become relatively similar due to the thermal ionization of local energy levels, as illustrated in Figure 16.

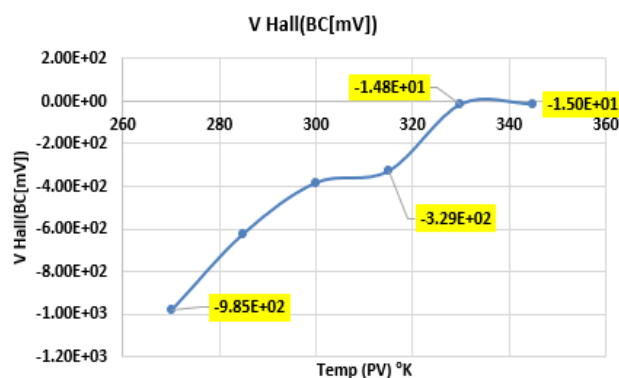


**Fig. 16.** Hall potential changes for the electrode (BC) with temperature changes.

At temperatures above 320 °K, the values continue to approach zero or stabilize at relatively small values, indicating that the transport has become subject to a combined contribution from both types of carriers, with the influence of local states associated with the grain boundary diminishing. This behavior reflects a thermal shift in the transport mechanism, rather than a quantum phase transition, given the high temperature compared to the Landau quantization energy at the applied magnetic field.

### 3.13.3 Changes in the AC electrode

Measurements between the AC electrodes showed relatively small values for the Hall potential compared to the other directions, with a gradual change in the signal within the range (300–320 °K). The small absolute value of the Hall potential suggests a possible convergence of electron and hole concentrations in the path between these electrodes, supporting the two-carrier transport hypothesis. The reversal of the thermal signal in this direction can be explained by the presence of a non-uniform distribution of local states or a difference in the grain boundary density along the current path between A and C in nanomaterials. Spatial structural variation leads to local differences in carrier density and mobility, which is directly reflected in the measured value and signal of the Hall modulus, as shown in Figure 17.

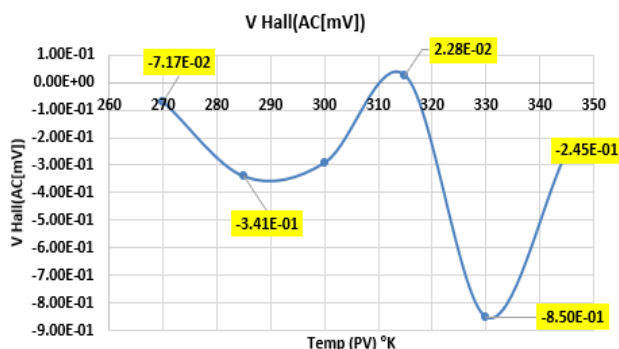


Fig. 17. Changes in the AC electrode with temperature.

The small values of the Hall potential may also reflect a significant contribution from magnetoresistance mixing due to the geometric asymmetry of the sample or the uneven distribution of the current under the influence of the magnetic field. Therefore, behavior in this direction is a clear indicator of the transport sensitivity of MoS<sub>2</sub> nanostructures to the microstructure and structural heterogeneity.

### 3.13.4 Hall potential change for the electrode (CD)

For measurements between the electrodes (CD), the data showed negative Hall potential values across most of the studied thermal range, with a gradual and regular change as the temperature increased, and no clear signal reversal. This behavior indicates the dominance of electrons as the primary carriers in this direction, with a smooth thermal transport mechanism, as illustrated in Figure 18.

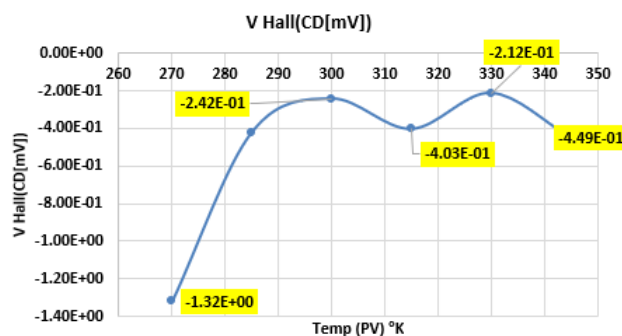


Fig. 18. Hall potential changes for the electrode (CD) with temperature change.

The absence of signal reversal in this pathway suggests that the electron concentration remains higher than the hole concentration within the entire thermal range. This indicates that the nanostructure between these two electrodes may contain a higher density of sulfur voids or electron-donating impurities compared to the other directions. Furthermore, the gradual change without any sharp jumps supports the conclusion that the system does not undergo a quantum phase transition, but rather a gradual redistribution of carriers due to thermal ionization. This trend likely represents a more structurally homogeneous region within the sample, where the effect of granular boundaries is less pronounced compared to other trends.

### 3.13.5 Changes in the hall potential for the electrode (DA)

Measurements between the electrodes (DA) show a clear change in the Hall potential signal with increasing temperature. At 320 °K, the value is negative, indicating the dominance of electrons as the primary charge carriers in this thermal range. This behavior is attributed to the sulfur-donating nature of the sulfur vacancies in MoS<sub>2</sub>, which generate energy levels close to the conduction band. As the temperature rises to approximately 300 °K, the Hall potential approaches zero, as shown in Figure 19.

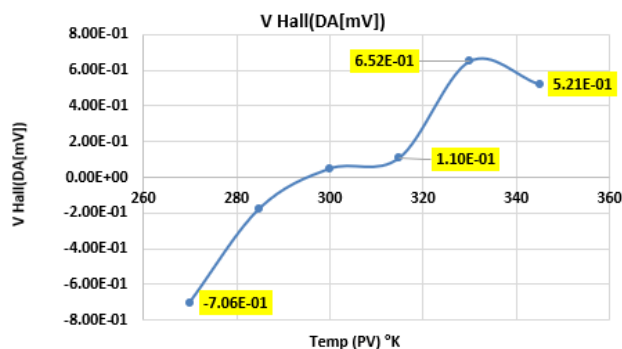
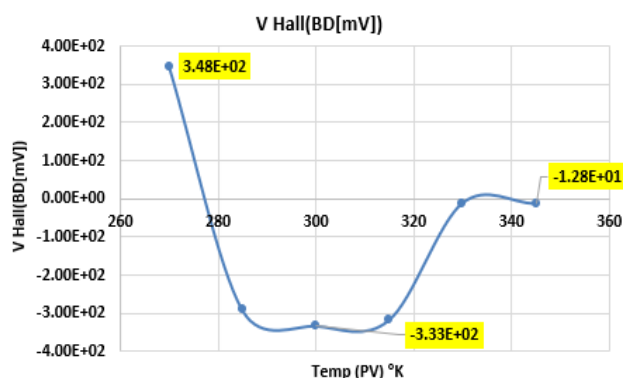


Fig. 19. Changes in the Hall potential for the electrode (DA) with temperature.

The signal then shifts to positive values and reaches an almost positive maximum value in the range of 325–335 °K. This signal reversal reflects a transition from a single-carrier (electronic) transport system to a two-carrier transport system, where the contribution of holes increases due to the thermal ionization of local or surface states in nanomaterials. The grain boundaries play an important role in determining the nature of the transport; they can act as energy barriers at low temperatures. Its effect then gradually decreases with increasing temperature, allowing for a greater contribution from charge carriers. Therefore, the gradual change in (DA) indicates a thermal shift in the transport mechanism from localized, defect-bound transport to more diffuse transport.

### 3.13.6 Hall potential change for the BD electrode

Measurements between the BD electrodes show more pronounced behavior compared to the DA direction. At 270 °K, the Hall potential is positive and relatively large, indicating hole dominance in this pathway. However, a slight increase in temperature leads to a rapid reversal of the signal towards negative values, with a clear minimum value in the range of 325–335 °K, as shown in Figure 20.



**Fig. 20.** Hall potential changes for the BD electrode with temperature change.

This behavior indicates the high sensitivity of the pathway between B and D to thermal changes, possibly reflecting a localized structural difference such as:

- Variation in grain boundary density,
- Variation in defect distribution,
- Asymmetry in nanolayer thickness.

The sharp decrease in the Hall potential followed by its gradual return to zero at higher temperatures supports the hypothesis of a bicarrier transport system in this direction, where the electron-to-hole ratio changes significantly with temperature. Furthermore, the figure is not The linearity of the curve indicates that transport is not governed by an ideal zonal mechanism, but is influenced by local conditions and scattering at the granular boundaries.

### 3.13.7 Hall average potential

Analyzing the Hall average potential is an important step to reduce the effects of local heterogeneity. The average curve exhibits a general behavior characterized by:

- Clearly negative values at low temperatures,
- Reaching a minimum value in the range (280–300 °K),
- Then a gradual rise towards zero at (330–345 °K).

This general behavior indicates that electrons are the dominant carriers at low temperatures, while increasing temperature reduces the difference between electron and hole concentrations, causing the Hall effect to approach zero, as shown in Figure 21.

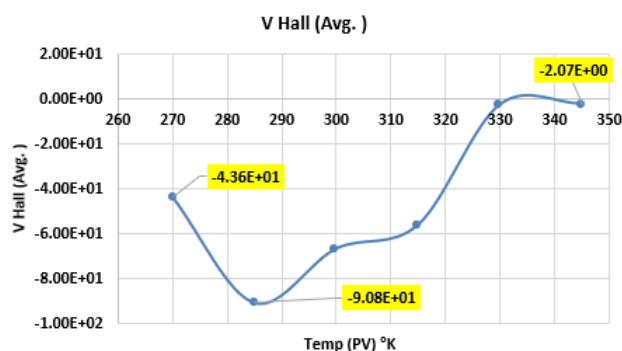


**Fig. 21.** Changes in the average Hall potential with temperature.

The gradual approach to zero without abrupt jumps or quantum plateaus confirms that the system does not enter a quantum Hall phase, but rather undergoes a gradual thermal transfer in the transport mechanism. Since the applied magnetic field (0.5 T) is insufficient to induce significant Landau quantization at temperatures close to room temperature, the observed behavior reflects a thermal redistribution of carriers within a heterogeneous nanostructure.

#### 4. DISCUSSION

1. The presence of three distinct thermal transport systems: The results showed a clear transition from a localized transport system dominated by surface states and defects at low temperatures, to a thermally activated system in the intermediate range, and then to a diffusion transport system limited by phonon scattering at higher temperatures.
2. A thermal transport region near 300 °K where a sharp decrease in carrier density, a possible reversal in the Hall effect signal, and a nonlinear change in mobility and resistivity were observed, indicating a shift in the dominant carrier type and the emergence of a two-carrier transport system.
3. The absence of evidence for a quantum Hall effect: Despite the observation of clear changes in the Hall potential, the lack of quantum plateaus or sharp phase jumps confirms that the observed phenomena are thermally transitional in nature and not quantum phase transitions. This confirms that quantum transitions are expected only at much lower temperatures.
4. Spatial heterogeneity in the Hall response: The observed differences between directional measurements (AB, BC, AC, CD, BD, DA) indicate the influence of nanostructure, grain boundaries, defect distribution, and surface states on electron transport, supporting the hypothesis of multichannel transport.
5. Optimal thermal window for electronic performance: The mobility exhibited a maximum value near ( $\approx 285$  °K), representing a balance between carrier activation and low phonon scattering, suggesting an optimal thermal field for enhancing electronic performance in MoS<sub>2</sub> nanostructures.
6. Importance of nanostructure in determining the transport mechanism: The results confirm that the effects of low dimensions and an increased surface-to-volume ratio play a crucial role in determining the nature of the transport, as the effects of local states, phonon scattering, and carrier compensation intertwine to determine the overall electrical behavior.

#### 5. CONCLUSIONS

The present study demonstrates that the electrical transport properties of MoS<sub>2</sub> nanostructures exhibit a clear temperature dependence within the investigated range. Hall effect and electrical measurements indicate that charge transport is governed by the combined influence of structural defects, surface states, and phonon scattering mechanisms associated with the nanostructured morphology of the material. At lower temperatures, carrier localization caused by defects and grain boundaries leads to increased resistivity and reduced carrier mobility. As the temperature increases, thermal activation of charge carriers enhances conductivity and facilitates transport through more extended conduction states. The observed variations in Hall voltage and carrier concentration suggest the involvement of multiple types of charge carriers, reflecting the complex transport behavior of nanostructured MoS<sub>2</sub> compared with bulk materials. At higher temperatures, phonon scattering becomes the dominant factor limiting carrier mobility. Additionally, directional variations in the Hall response reveal spatial inhomogeneity within the sample related to defect distribution, grain boundaries, and nanosheet orientation. These findings highlight the important role of nanostructure-related effects and thermal activation in determining the electronic transport behavior of MoS<sub>2</sub>, supporting its potential for applications in nanoelectronic and sensing devices based on two-dimensional materials.

#### Acknowledgement

The author is grateful to Prof. Dr. Lama Alchabb, Prof. Dr. Qaisar AlYamani, and Dr. Abdul-dahir for their assistance in finalizing this study and for their valuable contributions to the physical insights presented in this paper.

#### REFERENCES

- [1] C. Wang, L. Cusin, C. Ma, E. Unsal, H. Wang, V. Girelli-Consolaro, V. Montes García, B. Han, S. Vitale, A. Dianat, A. Croy, H. Zhang, R. Gutierrez, G. Cuniberti, L. Chi, A. Ciesielski, and P. Samori, "Enhancing the carrier transport in monolayer MoS<sub>2</sub> through interlayer coupling with 2D covalent organic frameworks," *Advanced Materials*, vol. 36, no. 1, p. e2305882, 2024. doi: 10.1002/adma.202305882.

- [2] A. Garcia Ruiz and M. H. Liu, "Twisted bilayer MoS<sub>2</sub> under electric fields: A system with tunable symmetry," *Nano Letters*, vol. 24, no. 51, pp. 16317–16324, 2024. doi: 10.1021/acs.nanolett.4c04556.
- [3] Z. Cheng, S. He, X. Han, X. Zhang, L. Chen, S. Duan, S. Zhang, and M. Xia, "Improving electron mobility in MoS<sub>2</sub> field effect transistors by optimizing the interface contact and enhancing the channel conductance through local structural phase transition," *Journal of Materials Chemistry C*, vol. 12, pp. 2794–2802, 2024. doi: 10.1039/D3TC04605B.
- [4] S. E. Panasci, I. Deretzis, E. Schilirò, A. La Magna, F. Roccaforte, A. Koos, M. Nemeth, B. Pécz, M. Cannas, S. Agnello, and F. Giannazzo, "Interface properties of MoS<sub>2</sub> van der Waals heterojunctions with GaN," *Nanomaterials*, vol. 14, no. 2, p. 133, 2024. doi: 10.3390/nano14020133.
- [5] J. Xue, T. Xia, T. Li, J. He, S. Wang, N. Li, G. Zhang, X. Duan, *et al.*, "Room temperature solution processing of high mobility MoS<sub>2</sub> thin films," *Nature Communications*, vol. 16, no. 1, p. 11538, 2025. doi: 10.1038/s41467-025-66523-z.
- [6] S. Kim, A. Konar, W. Hwang, J. Lee, J. Lee, J. Yang, C. Jung, H. Kim, J. Yoo, J. Choi, Y. Jin, S. Lee, D. Jena, W. Choi, and K. Kim, "High-mobility and low-power thin-film transistors based on multilayer MoS<sub>2</sub> crystals," *Nature Communications*, vol. 3, p. 1011, 2012. doi: 10.1038/ncomms2018.
- [7] I. Tyulnev, Á. Jiménez Galán, J. Poborska, *et al.*, "Valleytronics in bulk MoS<sub>2</sub> with a topologic optical field," *Nature*, vol. 628, pp. 746–751, 2024. doi: 10.1038/s41586-024-07156-y.
- [8] Y. Kitaoka, A. Ueda, and H. Imamura, "Tuning the electronic and magnetic properties of MoS<sub>2</sub> bilayers by transition metal intercalation," *Journal of Magnetism and Magnetic Materials*, vol. 602, p. 172168, 2024. doi: 10.1016/j.jmmm.2024.172168.
- [9] X. Xu, L. Yang, Q. Gao, X. Jiang, D. Li, and B. Cui, "Type II MoSi<sub>2</sub>N<sub>4</sub>/MoS<sub>2</sub> van der Waals heterostructure with excellent optoelectronic performance and tunable electronic properties," *Journal of Physical Chemistry C*, vol. 127, no. 14, pp. 5552–5563, 2023. doi: 10.1021/acs.jpcc.3c00773.
- [10] Y. Yang, D. He, Y. Zhou, S. Wen, and H. Huang, "Electronic and surface modulation of 2D MoS<sub>2</sub> nanosheets for an enhancement on flexible thermoelectric property," *Nanotechnology*, vol. 34, no. 19, p. 195402, 2023. doi: 10.1088/1361-6528/acb94a.
- [11] A. K. Mandia, R. Kumar, S. C. Lee, S. Bhattacharjee, and B. Muralidharan, "Magneto transport in the monolayer MoS<sub>2</sub> material system for high performance field effect transistor applications," *arXiv preprint arXiv:2312.00378*, 2023. doi: 10.48550/arXiv.2312.00378.
- [12] S. Ghosh, J. Zhang, M. Wasala, P. Patil, N. Pradhan, and S. Talapatra, "Probing the electronic and optoelectronic properties of multilayer MoS<sub>2</sub> field effect transistors at low temperatures," *Nanomaterials*, vol. 13, no. 16, p. 2333, 2023. doi: 10.3390/nano13162333.
- [13] Y. Manzanares-Negro, J. Quan, M. Rassekh, M. Moaied, X. Li, P. A. Ares, J. J. Palacios, J. Gomez-Herrero, and C. Gomez-Navarro, "Low resistance electrical contacts to few layered MoS<sub>2</sub> by local pressurization," *2D Materials*, vol. 10, no. 2, p. 021003, 2023. doi: 10.1088/2053-1583/acc1f4.
- [14] H. AlHussein, J. AlSharr, and H. AlKhamisy, "MoS<sub>2</sub> nanostructures prepared by hydrothermal method and their impedance behavior," *Journal of Materials and Engineering*, vol. 2, no. 4, pp. 303–314, 2024. doi: 10.61552/JME.2024.04.008.
- [15] H. Wei, A. Tan, *et al.*, "Interface engineering-induced 1T-MoS<sub>2</sub>/NiS heterostructure for efficient hydrogen evolution reaction," *Catalysts*, vol. 12, no. 9, p. 947, 2022. doi: 10.3390/catal12090947.